Supplemental Data

Figure S1, Related to Figure 1

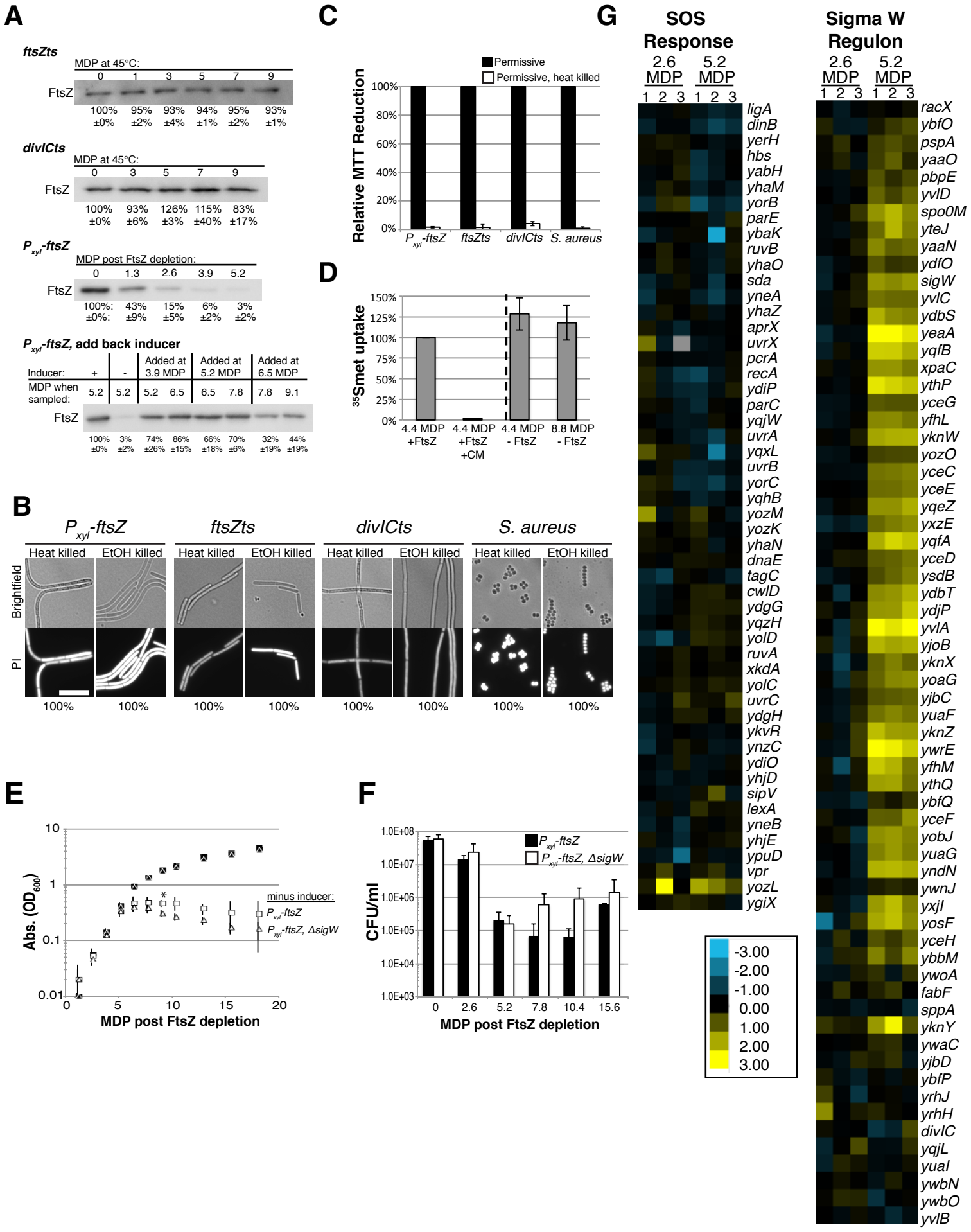

Figure S1, Related to Figure 1 – An extended block in cell division leads to a growth arrest and entry into a permanent, quiescent state at the Point of No Return (PONR).

A. Quantitative immunoblots of FtsZ levels in *ftsZts, divICts,* and P_{xyl}-*ftsZ* cells blocked for division for the indicated MDP. P_{xyl}-*ftsZ* cells were also subjected to immunoblotting when inducer was added back before (3.9 MDP), at (5.2 MDP) and after (6.5 MDP) the PONR. Intensity of the FtsZ bands was quantified with ImageJ and FtsZ levels at 0 MDP (permissive conditions) were set to 100%. Total protein per lane as measured by Ponceau staining was used as a loading control. Averages ±SD are shown below each blot, n=3.

B. All dead cells are PI positive. Cells for each strain were either heat killed at 80°C or killed with ethanol and imaged. Bar = 5 μm.

C. Heat killed cells do not reduce MTT. MTT reduction levels of cells in permissive conditions were set to 100%. Error bars = SD, n = 3.

D. Protein synthesis of P_{xyl}-*ftsZ* cells as measured by incorporation of ^{35}S-methionine. Error bars = SD, n = 3.

E. *sigW* deletion in P_{xyl}-*ftsZ* cells does not alter the timing of the PONR, but increases cell lysis and moderately increases plating efficiency after the PONR. (A) P_{xyl}-*ftsZ* (squares) and P_{xyl}-*ftsZ, ΔsigW* (triangles) were grown with and without xylose (closed and open symbols, respectively) and growth was monitored by OD_{600}. n=3. Error bars represent standard deviation. [*] indicates a statistically significant change between the P_{xyl}-*ftsZ* and P_{xyl}-*ftsZ, ΔsigW* strains grown in the absence of xylose (open symbols) as indicated by a Student's t-test, P=0.03. (B) P_{xyl}-*ftsZ* (black bars) and P_{xyl}-*ftsZ, ΔsigW* (white bars) were grown without xylose (-FtsZ) for the indicated MDPs and then plated in the presence of xylose (permissive conditions). CFU/ml is normalized to an OD_{600} of 0.5. n=3. Error bars represent standard deviation.

F. A heat map shows the majority of the genes in the SOS response – which is activated upon DNA damage – are not induced significantly or reproducibly before or at the PONR. A heat map of the Sigma W regulon shows the majority of genes in this regulon are induced at the PONR, 5.2 MDP post FtsZ depletion. Transcript levels for 3 replicates are represented as the fold change for FtsZ depleted cells as compared to FtsZ+ cells before the PONR at 2.6 MDP and at the PONR at 5.2 MDP. Transcript levels are indicated by color such that high levels are yellow and low levels are blue.

Figure S2, Related to Figure 1

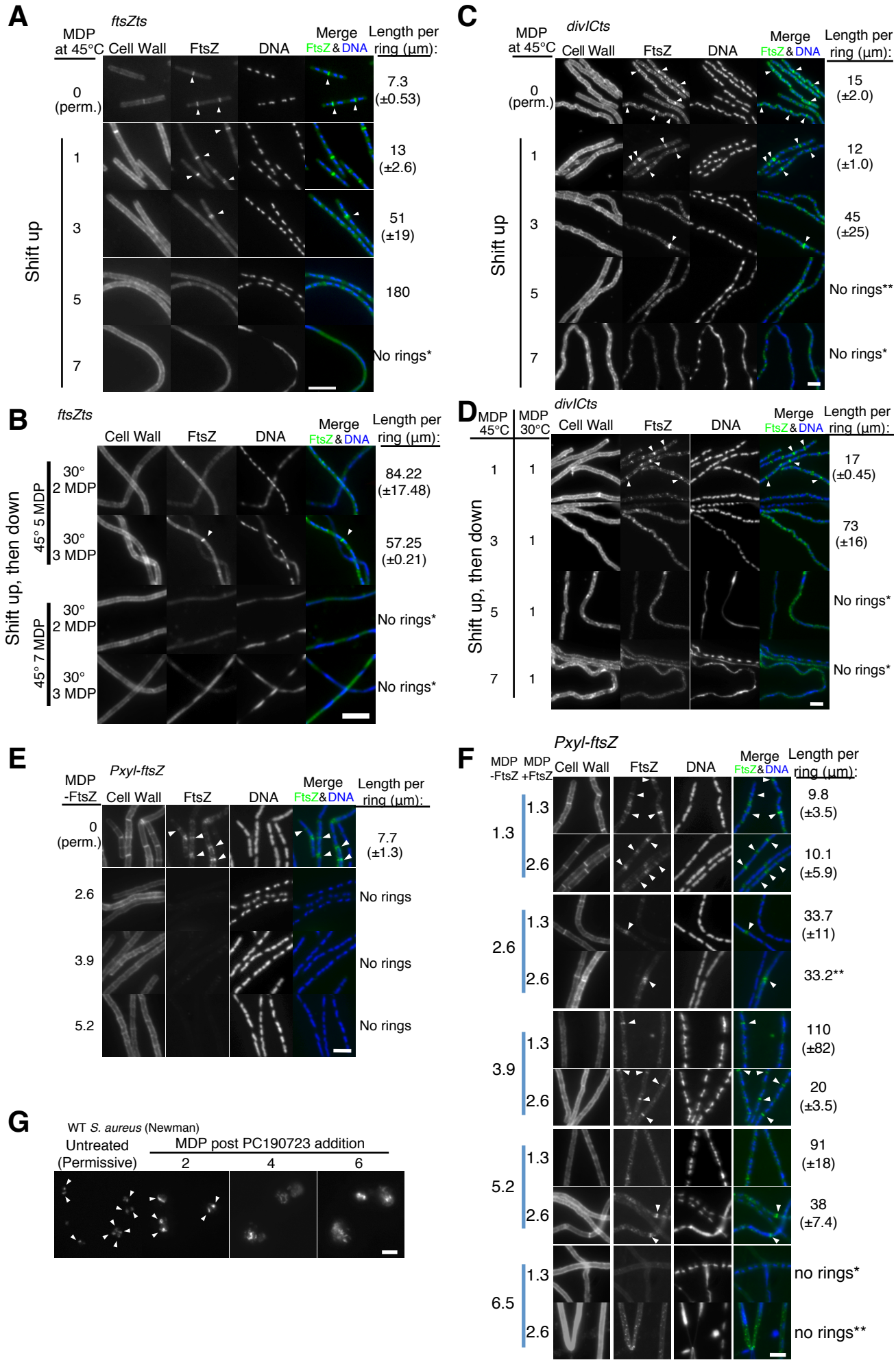

Figure S2, Related to Figure 1 – Cells subjected to a prolonged block in division cannot form new FtsZ rings after the PONR, consistent with a terminal cell cycle arrest.

A-F. Cell wall (WGA), FtsZ (FtsZ-GFP or immunolabelled FtsZ) and DNA (DAPI) are shown. Length-per-ring and nucleoid ratios were calculated by dividing total cell length by the number of FtsZ rings and nucleoids, respectively. Average ±SD are shown, n=3-4. ~200 wild-type cell lengths were measured per replicate. [No rings* and **] indicates experiments in which at least one replicate contained no observable FtsZ rings so an average could not be calculated. When the total length and total rings from the 3 replicates were compiled, [**] indicates a composite length-per-ring ratio of 183 and [*] indicates a composite length-per-ring ratio greater than 1500 μm.

A. Extant FtsZ rings remain in *ftsZts* cells blocked for division but new ones are not formed. Rings are not observed after the PONR.
B. *ftsZts* cells were cultured under nonpermissive conditions for 5 and 7 MDP prior to a shift to permissive conditions for an additional 2 or 3 MDP.
C. *divIC* cells initially exhibit a higher length-per-ring ratio. Existing rings remain after a shift to nonpermissive conditions but no new rings form after 3 MDP.
D. *divIC* cells shifted up to nonpermissive for 1, 3, 5 or 7 MDP before being shifted to permissive for 1 MDP. Rings cannot form when downshifted after 3 MDP at nonpermissive.
E. P_{xyl}-*ftsZ* cells lose FtsZ ring forming ability after inducer is washed out.
F. P_{xyl}-*ftsZ* cells can form rings if inducer is added back before the PONR (5.2 MDP), but cannot form rings if inducer is added back after the PONR at 6.5 MDP.
G. FtsZ rings remain in *S. aureus* treated with PC190723 up to 2 MDP, after which time rings are no longer observed.

Figure S3, Related to Figure 2

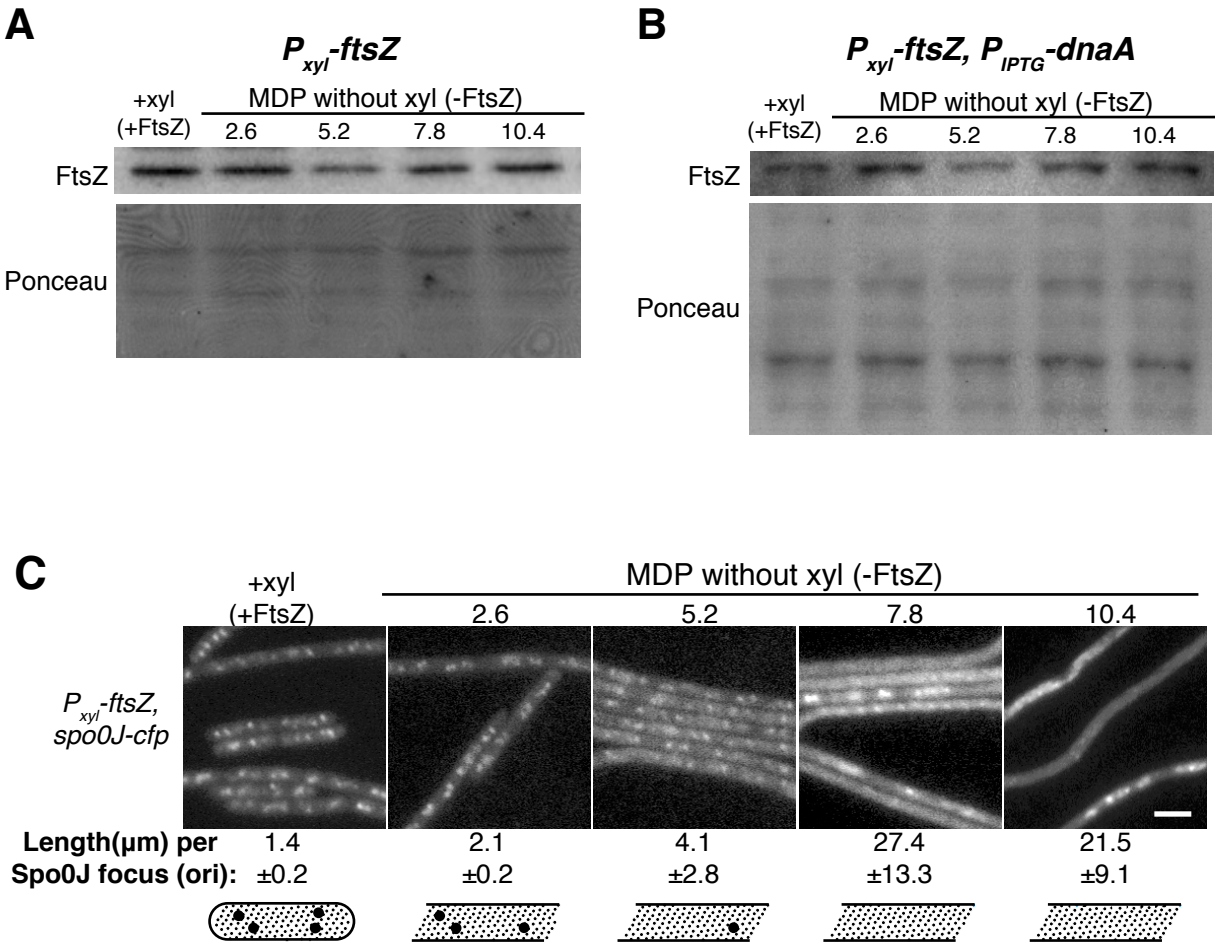

Figure S3, related to Figure 2 – A modest increase in DnaA levels is not sufficient to bypass the DNA replication arrest in cells subjected to an extended block in division.

A-B. Quantitative immunoblotting of DnaA in P_{xyl}-*ftsZ* (A) or P_{xyl}-*ftsZ,* P_{IPTG}-*dnaA* (B) cells blocked for division. Before blotting for DnaA, the blot was subjected to Ponceau staining to label total proteins for use as a loading control. A portion of the Ponceau stain is shown below each blot. For each of 3 experimental replicates, the DnaA levels were measured in ImageJ and normalized to measurements of the total protein from the Ponceau staining.

C. CFP-Spo0J foci disappear and staining becomes diffuse following a division block. Images of P_{xyl}-*ftsZ, CFP-spo0J* cells where replication is blocked and origins are labeled with CFP-Spo0J. The average length per CFP-Spo0J focus ±SD is indicated below the images along with a cartoon illustrating representative Spo0J-cfp staining. n = 3, ~200 cell units were scored per replicate. (A-B, E) Bars = 5 μm.

Figure S4, Related to Figure 3

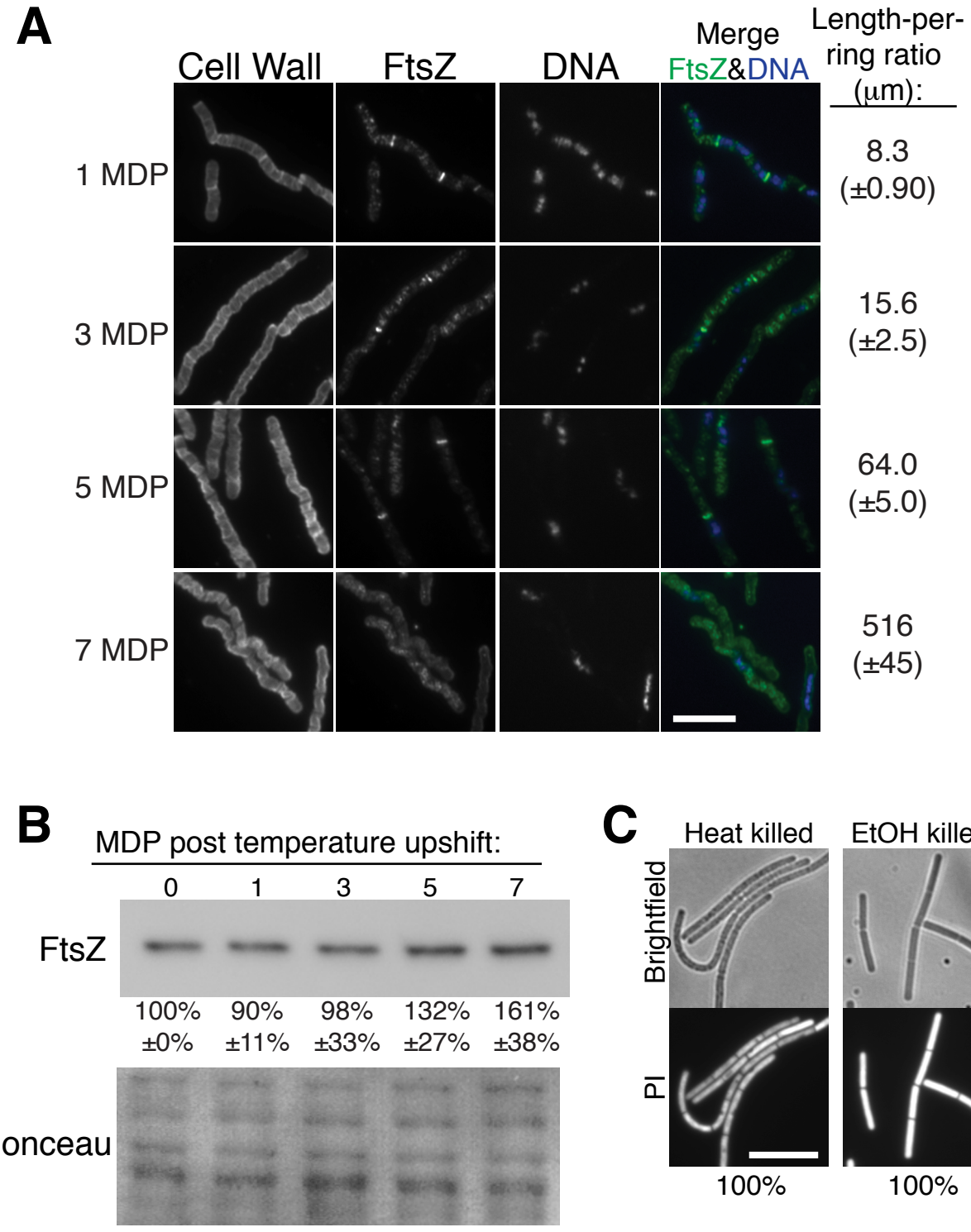

Figure S4 – *dnaBts* cells are refractile to FtsZ assembly when shifted to permissive conditions after the PONR.

A. Cells are refractile to FtsZ assembly after the PONR during a block in DNA replication initiation. *dnaBts* cells were cultured for 1, 3, 5, and 7 MDP at nonpermissive conditions before being shifted to permissive conditions for an additional MDP. Length per-ring ratios were calculated by dividing total cell length by the number of FtsZ rings. The average and SD of 3 replicates are shown.
B. FtsZ levels following a shift to nonpermissive conditions for the indicated MDP were measured using quantitative immunoblotting. 0 MDP was set to 100%. The average and SD are below the blot. Ponceau staining of total protein was used as a loading control (as described in Figure S3).
C. *dnaBts* cells were grown in permissive conditions, killed with heat or ethanol treatment, and subjected to PI staining. All killed cells stained with PI.

Table S1: Strains used in this paper

Strain	Genotype	Mass Doubling Period (MDP) (min)				Ref.
		30°C LB	37°C LB	45°C LB	$S_{750}G^2$ mod. media 37°C	
JH642 Background						
JH642 (PL522)	*Wild type*		23			[S1]
PL2084	*thrC*::P_{xyl}-*ftsZ MLS, ftsZ*::*spc, xylA*::*tet*		23		37	[S2]
PL642	*ftsZ*::*ftsZ-gfp cm*	34		17		[S3]
PL3482	*purA*::P_{rpmH}-*lacO-dnaA-lacI-cat, thrC*::P_{xyl}-*ftsZ MLS, ftsZ*::*spc, xylA*::*tet*		23			This work
PL3457	*pelB*::P_{soj}-*cfp(d)-spo0J(parS*)(cat), thrC*::P_{xyl}-*ftsZ MLS, ftsZ*::*spc, xylA*::*tet*		21			This work
HA184	*sigW*::*kan, thrC*::P_{xyl}-*ftsZ MLS, ftsZ*::*spc, xylA*::*tet*		23			This work
PL523	*dnaB134ts zhb*::*83*::*Tn917*	39.4		23		[S4]
PY79 Background						
PL146	*divIC*::*pPL27 spc*	46		25		[S5]
S. aureus Newman Background						
PL3056 (Newman)			36			[S6]
PL3068 (SEJ2)	*spa*::*erm*		36			[S7]
HA46	*ftsZ*::P_{spac}-*ftsZ-erm*		60			This work
B. subtilis and *S. aureus* strains used in strain construction						
PL3466 (NIS2020)	*purA*::P_{rpmH}-*lacO-dnaA-lacI-cat*					[S8]
PL3440 (BNS1762)	*pelB*::P_{soj}-*cfp(d)-spo0J(parS*)-cat*					[S9]
PL3211 (HB0042)	*sigW*::*kan*					[S10]
PL3037 (RNpFtsZ-1)	*RN4220, ftsZ*::P_{spac}-*ftsZ-erm*					[S11]

Table S2 - Genes upregulated 2-fold at the PONR (5.2 MDP)

SigW regulon members upregulated more than 2-fold at 5.2 MDP post FtsZ depletion			**Other genes (non SigW regulon) upregulated more than 2-fold at 5.2 MDP post FtsZ depletion**		
	5.2 MDP 2^x	Gene function (from Bsubcyc)		5.2 MDP 2^x	Gene function (from Bsubcyc)
fosB	2.100	metallothiol transferase	*bioK*	1.296	lysine-8-amino-7-oxononanoate aminotransferase
rsiW	1.297	anti-sigma(W) factor	*floT*	1.605	putative flotillin-like protein
sigW	1.746	RNA polymerase, σW	*manR*	1.207	transcriptional antiterminator
spo0M	1.840	sporulation-control gene	*motA*	1.167	motility protein A; MotA component of the stator flagellum complex
xpaC	1.653	putative phosphatase	*mtlA*	2.001	phosphotransferase system (PTS) mannitol-specific
yaaN	1.334	conserved hypothetical protein	*mtlD*	3.063	mannitol-1-phosphate dehydrogenase
yceC	1.439	putative stress adaptation protein	*vmlR*	1.197	ATP-binding cassette efflux transporter
yceD	1.212	putative stress adaptation protein	*yczI*	1.094	hypothetical protein
yceE	1.352	putative stress adaptation protein	*ydcC*	1.921	putative lipoprotein
yceF	1.322	putative stress adaptation transporter	*ydjG*	2.310	putative phage replication protein
ydbS	1.761	conserved hypothetical protein	*ydjH*	2.209	conserved hypothetical protein
ydbT	1.834	conserved hypothetical protein	*yjdH*	1.483	hypothetical protein
ydjP	2.903	putative peroxydase	*yocL*	1.318	hypothetical protein
yeaA	3.078	conserved hypothetical protein	*yozL*	1.425	conserved hypothetical protein
yfhL	1.539	SdpC immunity factor	*yqaL*	1.072	putative DNA-binding protein; skin element
yfhM	1.965	putative hydrolase	*yqeZ*	1.832	putative membrane bound hydrolase
yjbC	1.071	putative thiol oxidation management factor; putative acetyltransferase	*yqfA*	2.296	conserved hypothetical protein
yjoB	1.986	ATPase possibly involved in protein degradation	*yqfB*	2.297	conserved hypothetical protein
yknW	2.040	putative permease	*yqfC*	1.409	conserved hypothetical protein
yknX	1.269	putative efflux permease	*yqfD*	1.535	stage IV sporulation protein
yknY	1.881	putative ABC transporter (ATP-binding protein)	*yqfQ*	1.056	conserved hypothetical protein
yknZ	1.975	putative permease	*yrzI*	1.739	conserved hypothetical protein
yoaF	1.963	hypothetical protein	*ytfJ*	1.084	conserved hypothetical protein
yoaG	1.490	putative permease	*yuaF*	1.421	putative membreane integrity integral inner membrane protein
yobJ	1.686	hypothetical protein	*yvdS*	1.015	putative membrane protein
ysdB	1.209	conserved hypothetical protein	*yvkC*	1.351	putative phosphotransferase
yteJ	1.633	putative integral inner membrane protein	*yvlA*	2.053	conserved hypothetical protein
ythP	2.497	putative ABC transporter (ATP-binding protein)	*yvlC*	1.275	putative regulator (stress mediated)
ythQ	1.708	putative ABC transporter (permease)	*yvlD*	1.052	putative integral inner membrane protein
ywrE	2.773	conserved hypothetical protein	*yxjH*	1.289	putative methyl-tetrahydrofolate methyltransferase
yxjI	1.855	conserved hypothetical protein	**Genes in SigW regulon not upregulated more than 2-fold:**		
yxzE	1.459	putative bacteriocin	*sppA, yceH, pspA, yqeZ-floA-yqfB, bcrC, ywbN, ywaC, yceG, spx, fabF, divIC, fatR, ybfO, racX, yvlA-yvlB-yvlC-yvlD, ybfP, ydjO, yrhJ, ywnJ, ybfQ, pbpE, yqjL, ywbO, yrhH, yuaF-floT-yuaI, yozO*		

Supplemental experimental proceedures:

Bacterial strains, media and growth conditions. All strains and their genotypes are listed in Table S1. *B. subtilis* strains are derivatives of JH642 [S1] or PY79 [S12]. *S. aureus* strains are derivatives of *S. aureus* strain Newman [S6, S7]. Strain construction as described previously [S13] using genomic DNA from NIS2020 [S8], BNS1762 [S9] or HB0042 [S10]. Unless otherwise noted, *B. subtilis* strains were grown in Luria Broth (LB). *ftsZts* (PL642) was maintained in chloramphenicol at 5 μg ml^{-1}. *S. aureus* strains were grown in Tryptone Soy Broth (TSB) with 10 μg/ml of erythromycin when needed. To block cell division, P_{xyl}-*ftsZ* and derivative strains (PL2084, PL3482, PL3457, HA184) were grown to mid-exponential phase (OD600 0.2-0.5) with 0.5% xylose, washed twice in LB and backdiluted to a calculated OD600 of 0.004. *ftsZts* (PL642), *divICts* (PL146), and *dnaB134ts* (PL523) were maintained in LB at 30°C and backdiluted into LB medium at a calculated OD600 of 0.0075 (*ftsZts* and *dnaB134ts*) and 0.03 (*divICts*) at 45°C. *S. aureus* Newman was grown to mid-exponential phase in Tryptic Soy Broth (TSB) and backdiluted to an OD_{600} of 0.01 with 1 μg ml^{-1} PC190723 or 0.1% DMSO (vehicle). Newman P_{IPTG}-*ftsZ* (HA46) was grown to mid-exponential phase with 0.5 mM IPTG, washed twice in TSB, and backdiluted to an OD_{600} of 0.05 with and without IPTG.

Propidium Iodide Staining. Propidium iodide (PI) was added to cell cultures at a final concentration of 100 nM and cells were incubated for 10 minutes at room temperature. Cells were spotted on a 1% agarose pad and imaged using a 40X phase objective to visualize total cells and with a red fluorescent filter to visualize propidium iodide incorporation. For *B. subtilis* strains, we calculated the fraction of PI stained cells by

dividing the total PI positive cell length by the length of all cells visible on the phase image. For *S. aureus* strains, the fraction of PI stained cells was calculated by dividing the number of PI stained cells by the total cell count. Heat killed (80°C for 20 minutes) and ethanol treated cells were used as positive controls. Ethanol treated cells were suspended in a final concentration of 70% ethanol, cells were pelleted and resuspended in LB before PI staining.

EdU staining of newly replicated DNA. EdU staining was performed using the Invitrogen Click-iT EdU Alexa fluor 488 imaging kit C10083 [14, 15]. Cells were blocked for division by removing xylose in P_{xyl}-*ftsZ* cells or by adding 1 mg ml^{-1} PC190723 to *S. aureus* for the indicated MDP. EdU was added to a final concentration of 30 μg ml^{-1} and cells were incubated for 15 minutes at 37°C. Cells were fixed, washed with 1.0 ml PBS, resuspended in 100 μl of 2 mg ml^{-1} lysozyme in GTE (*B. subtilis*) or 20 μg ml^{-1} lysostaphin (*S. aureus)* and incubated for 3 minutes at room temperature. Cells were then washed with 1.0 ml PBS, the cell pellet was resuspended in 200 μl Click-iT reaction cocktail and incubated at room temperature in the dark for 30 minutes. Cells were washed 2 times in 1.0 ml PBS, resuspended in 1.0 ml PBS and spotted on 1% agarose pads. Cells were imaged with the 100X objective both in bright field and with a GFP filter. For the GFP images, exposures were taken for 2.4 seconds for *B. subtilis* and 1 second for *S. aureus* and the images were all adjusted equally using Adobe Photoshop. ImageJ analysis was used to quantify EdU staining by averaging data from ~90 circles with an area of 52 pixels that were in the DNA-stained regions of the cell and subtracting background fluorescence.

Quantitative Immunoblotting. Quantitative immunoblotting was performed as previously described in Weart and Levin, 2003 [S2], except that cell lysates were prepared with a FastPrep machine for 4 pulses of 20 seconds at 6.0 m/s or by lysing cells with lysozyme and detergent. Gel loading was normalized to the sampling OD_{600} and controlled by Ponceau S staining after the transfer. Quantification of FtsZ-bands was performed with ImageJ software.

MTT reduction assay. The MTT reduction assay was performed as previously described [S16], with the following modifications. 200 µl of culture at an approximate OD of 0.2 was added to 20 µl of 5 mg/ml MTT in a pre-warmed 1.7 ml eppendorf tube. The tubes were incubated on a shaker at 37 degrees (30 or 45 degrees for the temperature sensitive strains) for 5 minutes. Cultures were then pelleted and the pellets were stored at -20°C. Pellets were resuspended in 1 mL DMSO and assayed in triplicate in a 96-well plate read at 550 nm. Cells without MTT label and heat-killed cells were used as a control.

Fluorescence microscopy. Fluorescence microscopy was as previously described [S11, S17]. The length-per-ring and per-nucleoid ratio was calculated by dividing the total cell length by the number of FtsZ rings or individual nucleoids, respectively.

^{35}S-methionine protein synthesis assay. PL2084 cells were grown to midexponential phase (OD600 = ~0.200) in a modified $S7_{50}$ G^2 media (1X $S7_{50}$ salts, 1X Metals, 1% glycerol, 0.1% glutamate, 0.06% -met, -thr Clontech yeast dropout media, 0.04% Trp, 0.04% Phe, 0.04% Thr). Cells were backdiluted with and without xylose in the modified $S7_{50}$ G^2 media to an OD_{600} of 0.01. As a control, 200 µg ml^{-1} chloramphenicol was added to induced cells 30 minutes before labeling. At the indicated mass doubling period (MDP), 200 microcuries of ^{35}S-methionine was added to 1 ml of culture and cells were

grown for 10 additional minutes at 37°C. Cells were washed 2 times with PBS, resuspended in 100 µl GTE + 2 mg/ml lysozyme and 1 µl AEBSF and incubated at 37°C for 15 minutes and then on ice for 15 minutes. SDS was added to a final concentration of 2% and the cells were incubated at 95°C for 5 minutes. Protein was precipitated by adding 25 µl ice-cold TCA and incubating 10 minutes at 4°C. The protein was pelleted, washed with ice-cold acetone, and dried. Protein was resuspended in 20 µl ddH_20 and pipetted onto a FilterMat. The dried filters were placed in vials with 3 ml scintillation fluid and ^{35}S-methionine incorporation was measured using a scintillation counter.

Marker frequency analysis. DNA proximal to the origin (*oriC*) or terminus (*ter*) was amplified by qPCR and *ori:ter* ratios calculated as previously described [S18]. Data were normalized to induced cells treated with 200 µg ml^{-1} chloramphenicol for 4 hours (*ori:ter* ratio =1). Because values can vary widely experiment to experiment although the general pattern remained the same (values for induced cells ranged from 3-7), the data were additionally normalized by setting the *ori:ter* ratio of induced PL2084 cells to its average value of 5.

Plating Efficiency Assays. Plating efficiency assays were performed by growing cells in nonpermissive conditions and then plating serial dilutions in permissive conditions. CFU/ml of the culture was determined and normalized to an OD_{600} of 0.5. For each strain, relative CFU/ml was calculated by setting the CFU/ml at permissive conditions to 100%.

Microarray analysis. Gene expression in FtsZ depleted cells was compared with mock-depleted cells that were grown with xylose. Gene expression was monitored at 2.6 MDP post FtsZ depletion and at 5.2 MDP post FtsZ depletion. RNA was isolated using a Qiagen RNeasy RNA isolation kit. The procedures for sample collection, reverse

transcription, labeling, hybridization, and analysis were performed as described previously [S19]. Microarray data were analyzed using SAM [S20]. Genes with significantly altered expression levels were identified at a false discovery rate (FDR) of <5%. Genes were hierarchically clustered using the program Cluster and plotted with TreeView software. The entire data set can be found on the GEO website through the GEO Series accession number GSE56753 (http://www.ncbi.nlm.nih.gov/geo/query/acc.cgi?acc=GSE56753).

References

S1. Perego, M., Spiegelman, G. B., and Hoch, J. A. (1988). Structure of the gene for the transition state regulator, *abrB*: regulator synthesis is controlled by the *spo0A* sporulation gene in *Bacillus subtilis*. Molecular Microbiology *2*, 689–699.

S2. Weart, R. B., and Levin, P. A. (2003). Growth rate-dependent regulation of medial FtsZ ring formation. J Bacteriol *185*, 2826–2834.

S3. Levin, P., Kurtser, I., and Grossman, A. (1999). Identification and characterization of a negative regulator of FtsZ ring formation in *Bacillus subtilis*. Proc Natl Acad Sci USA *96*, 9642–9647.

S4. Rokop, M. E., Auchtung, J. M., and Grossman, A. D. (2004). Control of DNA replication initiation by recruitment of an essential initiation protein to the membrane of *Bacillus subtilis*. Molecular Microbiology *52*, 1757–1767.

S5. Levin, P. A., and Losick, R. (1994). Characterization of a cell division gene from *Bacillus subtilis* that is required for vegetative and sporulation septum formation. J Bacteriol *176*, 1451–1459.

S6. Duthie, E., and Lorenz, L. (1952). Staphylococcal coagulase: mode of action and antigenicity. Journal of general microbiology *6*, 95–107.

S7. Stranger-Jones, Y., and Bae, T. (2006). Vaccine assembly from surface proteins of *Staphylococcus aureus*. Proc Natl Acad Sci USA *103*, 16942–16947.

S8. Ogura, Y., Imai, Y., Ogasawara, N., and Moriya, S. (2001). Autoregulation of the dnaA-dnaNOperon and Effects of DnaA Protein Levels on Replication Initiation in *Bacillus subtilis*. J Bacteriol *183*, 3833–3841.

S9. Sullivan, N. L., Marquis, K. A., and Rudner, D. Z. (2009). Recruitment of SMC by ParB-parS Organizes the Origin Region and Promotes Efficient Chromosome Segregation. Cell *137*, 697–707.

S10. Butcher, B. G., and Helmann, J. D. (2006). Identification of *Bacillus subtilis* SigmaW-dependent genes that provide intrinsic resistance to antimicrobial compounds produced by *Bacilli*. Molecular Microbiology *60*, 765–782.

S11. Pinho, M., and Errington, J. (2003). Dispersed mode of *Staphylococcus aureus* cell wall synthesis in the absence of the division machinery. Mol Microbiol *50*, 871–881.

S12. Youngman, P., and Perkins, J. (1983). Genetic transposition and insertional mutagenesis in *Bacillus subtilis* with *Streptococcus faecalis* transposon *Tn917*. Proc Natl Acad Sci USA *80*, 2305–2309.

S13. Harwood, C. R., and Cutting, S. M. (1990). Molecular biological methods for

Bacillus. Modern Microbiological Methods.

S14. Salic, A., and Mitchison, T. J. (2008). A chemical method for fast and sensitive detection of DNA synthesis in vivo. Proc Natl Acad Sci USA *105*, 2415–2420.

S15. Ferullo, D., Cooper, D., Moore, H., and Lovett, S. (2009). Cell cycle synchronization of *Escherichia coli* using the stringent response, with fluorescence labeling assays for DNA content and replication. Methods *48*, 8–13.

S16. Wang, H., Cheng, H., Wang, F., Wei, D., and Wang, X. (2010). An improved 3-(4,5-dimethylthiazol-2-yl)-2,5-diphenyl tetrazolium bromide (MTT) reduction assay for evaluating the viability of *Escherichia coli* cells. J Microbiol Methods *82*, 330–333.

S17. Levin, P. A. (2002). Light Microscopy Techniques for Bacterial Cell Biology. Methods in Microbiology *31*, 115–132.

S18. Hill, N. S., Kadoya, R., Chattoraj, D. K., and Levin, P. A. (2012). Cell size and the initiation of DNA replication in bacteria. PLoS Genet *8*, e1002549.

S19. Britton, R. A., Eichenberger, P., Gonzalez-Pastor, J. E., Fawcett, P., Monson, R., Losick, R., and Grossman, A. D. (2002). Genome-Wide Analysis of the Stationary-Phase Sigma Factor (Sigma-H) Regulon of *Bacillus subtilis*. J Bacteriol *184*, 4881–4890.

S20. Tusher, V. G., Tibshirani, R., and Chu, G. (2001). Significance analysis of microarrays applied to the ionizing radiation response. Proc Natl Acad Sci USA *98*, 5116–5121.